

Determination of curvature and twist by digital shearography and wavelet transforms

Tay, Cho Jui; Fu, Yu

2005

Tay, C. J., & Fu, Y. (2005). Determination of curvature and twist by digital shearography and wavelet transform. *Optics Letters*, 30(21), 2873-2875.

<https://hdl.handle.net/10356/92036>

<https://doi.org/10.1364/OL.30.002873>

This paper was published in [Optics Letters] and is made available as an electronic reprint with the permission of OSA. The paper can be found at the following URL on the OSA website: [<http://www.opticsinfobase.org/ol/abstract.cfm?URI=ol-30-21-2873>]. Systematic or multiple reproduction or distribution to multiple reproduction or distribution to multiple locations via electronic or other means is prohibited and is subject to penalties under law.

Downloaded on 20 Mar 2024 19:18:21 SGT

Determination of curvature and twist by digital shearography and wavelet transforms

Cho Jui Tay and Yu Fu

Department of Mechanical Engineering, National University of Singapore, 10 Kent Ridge Crescent, Singapore 119260

Received April 18, 2005; revised manuscript received June 11, 2005; accepted July 15, 2005

A new technique based on digital shearography for determining the transient curvature and twist of a continuously deforming object from a series of speckle patterns is presented. The intensity variation of each pixel is analyzed along the time axis by using a complex Morlet wavelet transform. The absolute sign of the phase variation is determined by introduction of a temporal carrier when the speckle patterns are captured by a high-speed camera. A high-quality spatial distribution of the deflection derivative is extracted at any instant without the need for temporal or spatial phase unwrapping. The continuous Haar wavelet transform is subsequently processed as a differentiation operator to reconstruct the instantaneous curvature and twist of a continuously deforming object. © 2005 Optical Society of America

OCIS codes: 100.7410, 120.5050, 120.6160, 110.6150.

The demand for higher quality and structural reliability necessitates better techniques for nondestructive evaluation of stresses in a structure. Optical methods such as holography and shearography¹ are of considerable interest because of their full-field and noncontact features. Among them, shearography²⁻⁵ allows direct measurement of surface displacement derivatives and is a practical method that has received wide industrial acceptance for nondestructive testing. However, the second derivatives of displacement are generally of more interest, as they are directly related to stresses in a structure. Several reports⁶⁻⁹ have described methods to obtain the curvature and twist by using shearography. Some of them were based on fringe counting, which suffers from the low visibility of fringes; others utilized phase shifting, which is not easily accomplished on a continuously deforming object. In this investigation a temporal wavelet transform^{10,11} is applied in digital shearography to obtain a high-quality first-derivative map; a continuous Haar wavelet transform is utilized to extract the second derivative of the displacements. Figure 1(a) shows a schematic layout of a digital shearography setup. A modified Michelson shearing interferometer^{3,12} is adopted as the shearing device.

Similar to a temporal Fourier transform,¹³ a temporal wavelet transform is also unable to analyze the part of the object where phase change is zero or to determine the absolute sign of the phase change. However, that difficulty can be overcome by the addition of a carrier frequency during the image-acquisition process.¹³ In this study, a temporal carrier is introduced by a shift in mirror M2 via a piezoelectric transducer stage [see Fig. 1(a)]. The carrier frequency is high enough to ensure that the phase change at any point on the object is in one direction only. When the shearing is in the y direction and with near-normal illumination and viewing conditions, the intensity variation of each pixel can be expressed as

$$I_{xy}(t) = I_{0xy}(t) + A_{xy}(t) \cos[\varphi_{xy}(t)] \\ = I_{0xy}(t) \left\{ 1 + V \cos \left[\phi_{0xy} + \phi_C(t) + \frac{4\pi}{\lambda} \frac{\partial w_{xy}(t)}{\partial y} \delta y \right] \right\}, \quad (1)$$

where $I_{0xy}(t)$ is the intensity bias of the speckle pattern, V is the visibility, ϕ_{0xy} is a random phase, $\phi_C(t)$ is the phase change due to the temporal carrier, and $w_{xy}(t)$ is the out-of-plane deformation of the object. At each pixel the temporal intensity variation is a frequency-modulated signal and is analyzed by a continuous wavelet transform. The continuous wavelet transform¹⁴⁻¹⁶ of a signal $s(t)$ is defined as its inner product with a family of wavelet functions $\psi_{a,b}(t)$:

$$W_S(a,b) = \int_{-\infty}^{+\infty} s(t) \psi_{a,b}^*(t) dt, \quad (2)$$

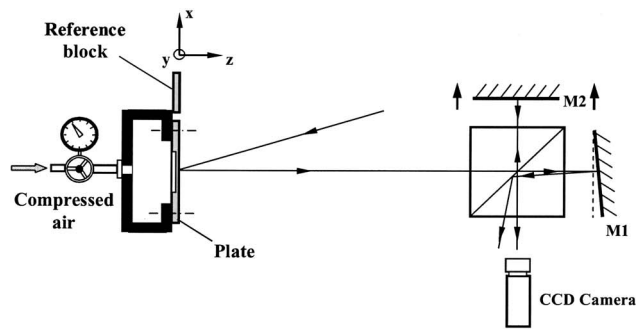
where

$$\psi_{a,b}(t) = \frac{1}{\sqrt{a}} \psi\left(\frac{t-b}{a}\right), \quad b \in \mathbb{R}, a > 0. \quad (3)$$

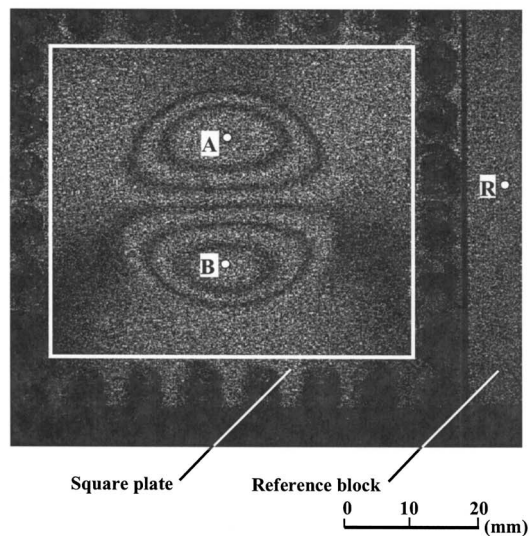
Here a is a scaling factor related to the frequency, b is the time shift, and $*$ denotes the complex conjugate. In this application the complex Morlet wavelet is selected as a mother wavelet:

$$\psi(t) = \exp(-t^2/2) \exp(i\omega_0 t). \quad (4)$$

Here $\omega_0 = 2\pi$ is chosen to satisfy the admissibility condition.¹⁴ The continuous wavelet transform expands a one-dimensional temporal intensity variation of certain pixels into a two-dimensional plane of scaling factor a (which is related to the frequency) and position b (which is the time axis). The trajectory of the maximum $|W_{xy}(a,b)|^2$ on the a - b plane is



(a)



(b)

Fig. 1. (a) Schematic layout of a digital shearography setup. (b) Typical shearography fringe pattern and area of interest.

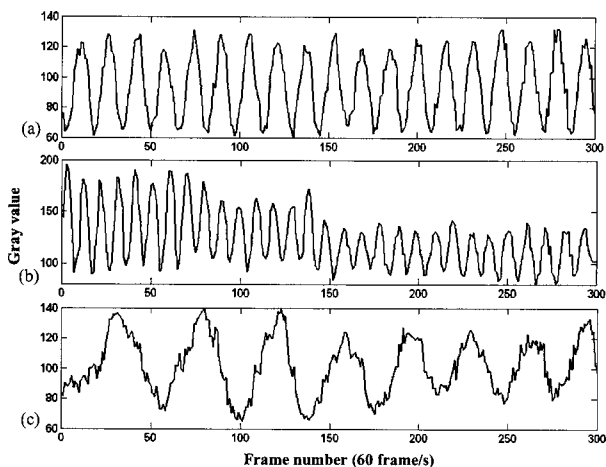


Fig. 2. Temporal intensity variations of (a) point R on the reference block and of (b) point A and (c) point B on the square plate.

called a ridge. The instantaneous frequency of signal $\varphi'_{xy}(b)$ is calculated as

$$\varphi'_{xy}(b) = \omega_0/a_{rb}, \quad (5)$$

where a_{rb} denotes the value of a at instant b on the ridge. The phase change $\Delta\varphi_{xy}(t)$ can be calculated by integration of the instantaneous frequency in Eq. (5), and a phase unwrapping procedure is not needed in the temporal and spatial domains. Subtracting the phase change $\Delta\phi_C(t)$ that is due to the temporal carrier, the absolute phase change representing $\partial w_{xy}/\partial y$ can be obtained on each pixel.

After phase retrieval by temporal wavelet analysis, a continuous Haar wavelet transform¹⁷ is applied spatially on the phase map at a certain instant to obtain the transient curvature and twist. The Haar function is the simplest wavelet, and a flexible differentiation operator

$$\psi(x) = \begin{cases} 1 & x \in [0, 1/2) \\ -1 & x \in [1/2, 1) \\ 0 & x \in \text{others} \end{cases}. \quad (6)$$

The wavelet coefficient obtained is the derivative of the signal. Different scaling factors a can be selected

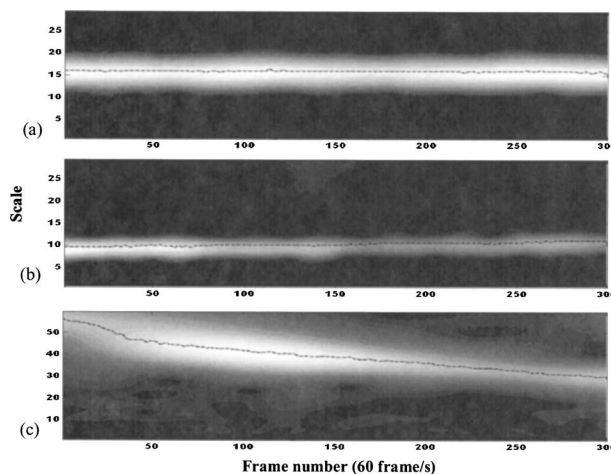


Fig. 3. Plot of the modulus of the Morlet wavelet transform at (a) point R, (b) point A, (c) point B.

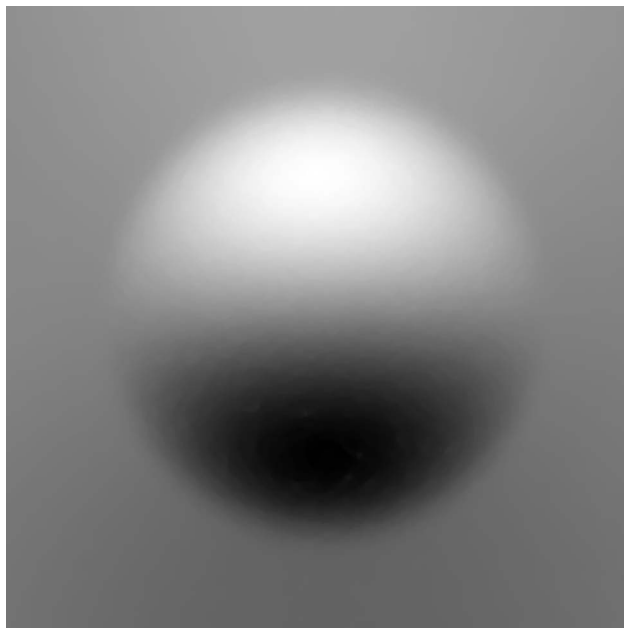


Fig. 4. Spatial phase distribution at $t=4$ s.

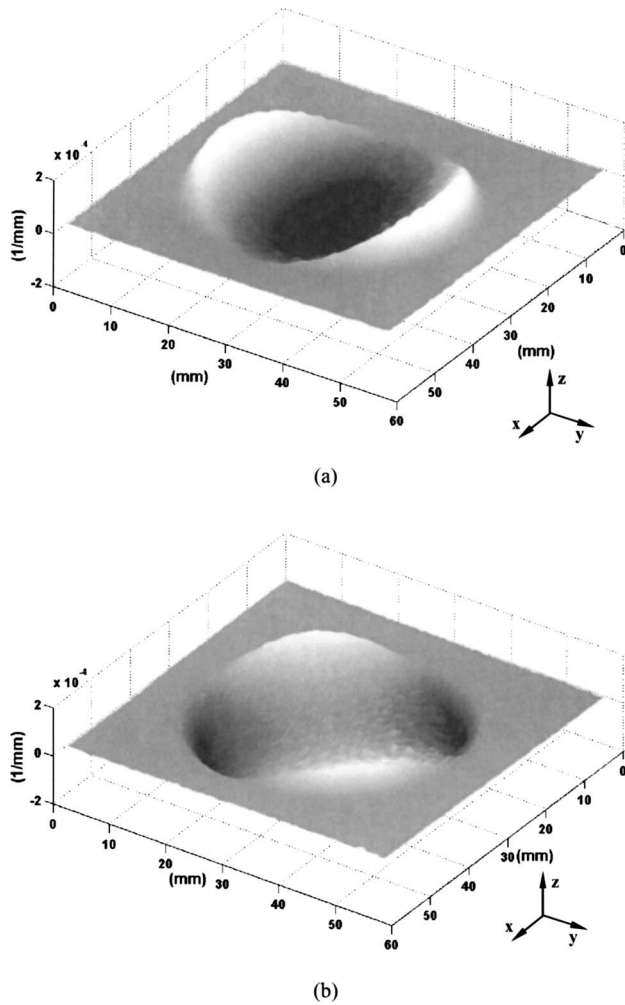


Fig. 5. Reconstructed values of (a) $\partial^2 w / \partial y^2$ and (b) $\partial^2 w / \partial x \partial y$ after a continuous Haar wavelet transform.

according to the extent of the noise. In this application, the continuous Haar wavelet transform is applied line by line in the x or y direction on the phase map.

The test specimen in this study is a square plate with a blind hole, clamped at the edges by rows of screws, loaded by compressed air and illuminated by a 35 mW He–Ne laser. To retrieve the phase change of the temporal carrier, a stationary reference block with a diffuse surface is mounted beside the object, and its image is captured along with the plate by a high-speed camera with an array size of 512×480 pixels. Figure 1(b) shows the typical shearography fringes of the test specimen with the reference block. The shearing distance δy is 3 mm, and 300 speckle patterns are processed pixel by pixel along the time axis. Figure 2 shows the intensity variations of a point R on the reference block and points of interest A and B on the plate. Different frequencies are observed at points A and B, as the phase changes at these two points are of opposite signs. Figure 3 shows the modulus of the Morlet wavelet transform on these points. The dashed curves show the ridge of the

wavelet transform where the maximum modulus is found. The temporal phase change (with carrier) at each point is obtained by integration, and its absolute phase change is thus obtained by subtraction of the carrier phase change. The combination of the phase change at each point at a certain instant results in an instantaneous spatial phase distribution that is proportional to the deflection derivative, in this case $\partial w / \partial y$. Figure 4 shows a high-quality phase map at an instant $t = 4$ s. It is worth noting that a 3×3 median filter is applied once on the phase map to remove ill-behaved pixels. A continuous Haar wavelet transform is then applied with a certain scaling factor a (in this application, $a = 20$) line by line in the y or x direction. The wavelet coefficients obtained represent the curvature $\partial^2 w / \partial y^2$ and the twist $\partial^2 w / \partial x \partial y$. Figure 5 shows three-dimensional plots of the curvature and twist obtained at instant $t = 4$ s.

This paper presents a novel method for retrieving the transient curvature and twist of a continuously deforming object by using a combination of digital shearography and the continuous wavelet transform. The proposed method is able to limit the influence of various noise sources and significantly improve the results in phase measurement. Because of the high quality of the phase map obtained, it is possible to perform a numerical differentiation process spatially. In addition, a continuous Haar wavelet transform is selected as a differentiation operator to eliminate the noise effect. Thus a good-quality transient curvature and twist can be obtained from a continuously deforming object.

Yu Fu's e-mail address is mpefuy@nus.edu.sg.

References

1. Y. Y. Hung, *Opt. Lasers Eng.* **26**, 421 (1997).
2. Y. Y. Hung, *Opt. Eng.* **21**, 391 (1982).
3. Y. Y. Hung, *Opt. Commun.* **11**, 132 (1974).
4. Y. Y. Hung, *Opt. Lasers Eng.* **24**, 161 (1996).
5. Y. Y. Hung, *Trends in Optical Non-Destructive Testing and Inspection* (Elsevier, 2000), Chap. 20.
6. C. J. Tay, S. L. Toh, H. M. Shang, and Q. Y. Lin, *Opt. Laser Technol.* **26**, 91 (1994).
7. C. J. Tay, S. L. Toh, H. M. Shang, and Q. Y. Lin, *Appl. Opt.* **34**, 2202 (1995).
8. P. K. Rastogi, *Opt. Lett.* **21**, 905 (1996).
9. F. S. Chau and J. Zhou, *Opt. Lasers Eng.* **39**, 431 (2003).
10. Y. Fu, C. J. Tay, C. Quan, and L. J. Chen, *Opt. Eng.* **43**, 2780 (2004).
11. Y. Fu, C. J. Tay, C. Quan, and H. Miao, *Appl. Opt.* **44**, 959 (2005).
12. J. A. Leendertz and J. N. Butters, *J. Phys. E* **6**, 1107 (1973).
13. C. Joenathan, B. Franze, P. Haible, and H. J. Tiziani, *Opt. Eng.* **37**, 1790 (1998).
14. I. Daubechies, *Ten Lectures on Wavelets* (Society for Industrial and Applied Mathematics, 1992), Chap. 2.
15. L. R. Watkins, S. M. Tan, and T. H. Barnes, *Opt. Lett.* **24**, 905 (1999).
16. J. Fang, C. Y. Xiong, and Z. L. Yang, *J. Mod. Opt.* **48**, 507 (2001).
17. J. Cao and Y. Sun, in *Proc. SPIE* **2536**, 57 (1995).